Airfoil Drag in Ideal Conditions

Zakary Steenhoek

This experiment aimed to test the drag on two standard airfoils in a wind tunnel under steady flow conditions. Analysis of the resulting drag was performed under ideal flow assumptions, and the resulting data was manipulated to compare the resulting C_d with the results from previous labs and technical writings.

I. Nomenclature

ρ	=	air density
$\forbidden{V}$	=	volume
n	=	molar mass
R	=	universal gas constant
T	=	temperature
U	=	internal energy
KE	=	kinetic energy
PE	=	potential energy
$C\forbidden{V}$	=	control volume
CS	=	control surface
$\hat{n}$	=	normal vector
∂	=	partial derivative
M	=	conversion factor
E	=	voltage
p_{static}	=	static pressure
p_{total}	=	total pressure
p_{gauge}	=	gauge pressure
p_{MM}	=	manometer pressure
V_∞	=	dynamic velocity
$\dot{m}$	=	mass time derivative
A_1	=	upstream cross-sectional area
A_2	=	downstream cross-sectional area
f	=	fan speed
p_1	=	upstream static pressure
p_2	=	downstream static pressure
δP	=	differential pressure across the test section
P_{atm}	=	absolute atmospheric pressure
V_1	=	upstream flow velocity
V_1	=	downstream flow velocity
c	=	dimensionless chord
α	=	angle of attack
C_p	=	pressure coefficient
C_l	=	lift coefficient
C_d	=	drag coefficient
C_x	=	x-force coefficient
C_z	=	z-force coefficient
L	=	lift
D	=	drag
$\bar{x}$	=	dimensionless x
$\bar{z}$	=	dimensionless z

x = x coordinate
z = z coordinate
p_i = static pressure
p_∞ = absolute pressure

II. Introduction

Just as in the last lab, lift and drag across a surface are arguably some of the the most important calculations in aerospace engineering. These values tell the engineer how the surface in question will affect the behavior and design of an aircraft. In this experiment, the drag force specifically was investigated further.

Previously, the drag found was simply a result of the pressure force, however, the true drag on an airfoil is much more complicated, and involves the pressure drag, the friction drag, and the induced drag. Here, the drag is found as a result of conservation laws, which should include a combination of both the pressure drag and the friction drag.

The induced drag is generally an unavoidable result of the lift that the airfoil creates, and is most prevalent at the the ends or at the wingtips of an airfoil. The design of this experiment limited the effects of induced drag by using an airfoil that spans the entire width of the testing section of the airfoil, which effectively simulates an infinitely long foil section, and does not include an 'end'. Measurements are taken from the flow over the foil near the center, such that boundary layer flow inconsistency near the edges of the section can be neglected. By using this data and calculating drag per unit width, this experiment can predict the total drag of an airfoil per unit width in steady flow with relative accuracy.

These results will finally be compared with the drag computed in the prior experiment to allow an analysis of the frictional drag, and how much of a role it plays in the total drag of an airfoil compared to just the pressure drag.

A. Objective

The goal of this test is first to determine the laboratory air density. This provides an important data point, from which wind-tunnel flow velocity can be determined as a function of pressure. This will be done differently than the prior experiments, as a more accurate pressure reading is necessary for accurate conservation law and control volume analysis. The same calculations are done, however instead of using the single reading for laboratory pressure and temperature, the data collected from the files will be manipulated to obtain accurate data as it changes throughout the process of the experiment.

The main objective of this experiment is to determine the effective total friction on an airfoil in steady flow. This will be done by using control volume analysis and conservation laws to determine how much external force is acting on the flow of fluid, which, according to newton's laws, is equal and opposite to the force acting on the airfoil. To maintain accuracy, the airfoils are set up such that they are at an angle of attach where they generate zero lift, meaning the resulting calculations of external force will include only the drag produced by the airfoil.

Finally, a comparison of the results obtained from the previous experiment will be done to determine how much significance skin drag has on the total drag force. This opens the door for analysis of different materials and the drag produced, and how to minimize the skin drag to design a more aerodynamically efficient airfoil and aircraft.

B. Assumptions

Assumptions are made in this experiment which make it possible to produce meaningful results without creating substantial error. These assumptions allow for simplicity in data collection and processing, and allow the use of some key physical laws. Assumptions made include the following:

1. Ideal Atmosphere

To determine the density of the laboratory air, the ideal gas law is used, which is only applicable to ideal gasses. The assumption is made that the atmosphere may be be treated as an ideal gas.

2. Incompressible & Uniform Flow

Methods to determine flow velocity through the test area apply the conservation of mass. The fluid flow is assumed to me uniform, and density of laboratory air is assumed to be constant, and therefore the term representing the change in mass inside the control volume w.r.t time evaluates to zero.

3. Inviscid Fluid

Methods to determine flow velocity through the test area apply the conservation of energy. The effects of viscous forces on the fluid are assumed to be negligible, and therefore energy loss can be neglected, and Bernoulli's equation may be applied.

C. Physical Laws

1. Ideal Gas Law

The first governing law in this experiment fundamental ideal gas law, Eq.(1) . This is a thermodynamic equation of state for an ideal gas, which relates physical properties and known constants.

$$p\forall = nRT \tag{1}$$

2. Bernoulli's Equation

The next governing law is the fundamental conservation of energy equation, Eq. (2), which states that the total energy of a system, consisting of the internal energy U, the kinetic energy KE, and the potential energy PE, remains constant.

$$U + KE + PE = const. \tag{2}$$

3. Mass Conservation

The next governing law is the fundamental conservation of mass, Eq.(3), which states that the change in mass inside a control volume w.r.t time plus the mass convected across the control surface must always sum to 0.

$$\frac{\partial}{\partial t}\int_{C\forall} \rho \, d\forall + \int_{CS} \rho(\vec{V} \cdot \hat{n}) \, dA = 0 \tag{3}$$

4. Error Propagation

The final governing equation is Gauss's formula for error propagation, Eq.(4), which describes the effect of uncertainty in a calculation as a function of the uncertainty in the variables involved, where i is the number of variables with uncertainty.

$$\delta y = \sqrt{\sum_i \left(\frac{\partial y}{\partial x_i}\delta x_i\right)^2} \tag{4}$$

D. Experimental Equipment

1. Hot Wire Anemometer

A hot wire anemometer **??** is a device used to measure the velocity of flowing fluid. It is a precision measurement device, and can detect minor changes in turbulent flow. It is based on the principle of maintaining a constant temperature by inducing a current through the wire in response to temperature changes. The wire temperature changes due to convective heat transfer out of the wire into the fluid, which is a function of flow velocity. The changes in voltage required to maintain a constant temperature are related to the fluid velocity as stated by King's law, Eq.(5):

$$V = E^m \cdot e^b \tag{5}$$

Where V is the velocity, E is the voltage difference, and m and b are constants of the power curve of V vs E.

2. Low-speed wind tunnel

A low speed wind tunnel[1] is a large lab machine with a fan, flow normalization, a test section, and related instrumentation. The tunnel used in this experiment is a closed tunnel, which circulates a constant volume of air through a ducting system using a fan. Before the test section, the cross-sectional area of the tunnel decreases, and according to Eq.(3), the velocity must increase. This closed system creates an optimal environment for aerodynamic testing. A general wind tunnel diagram is shown in Fig.1.

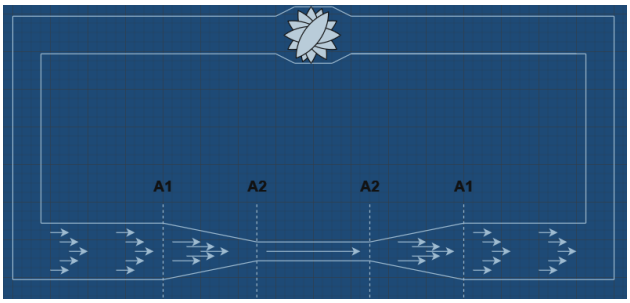

Fig. 1 General wind tunnel setup. Note the contraction area on the left-hand side, where the cross-sectional area reduces from A_1 to A_2.

3. NACA 0012 Airfoil

The NACA 0012 airfoil is a standardized airfoil shape defined by the National Advisory Committee for Aeronautics. It is a symmetric airfoil with no camber and a maximum 12% thickness to chord length ratio. The sample NACA 0012 airfoil used here has a chord c of $100mm$.

4. NACA 4412 Airfoil

The NACA 4412 airfoil is a standardized airfoil shape defined by the National Advisory Committee for Aeronautics. It is a non-symmetric airfoil with maximum 4% camber located 40% (0.4 chords) from the leading edge and a maximum 12% thickness to chord length ratio. The sample NACA 4412 airfoil used here has a chord c of $100mm$.

5. Absolute pressure transducer

An absolute pressure transducer[2] is a digital measurement device that measures pressure in the absolute range, i.e. from a zero-reference point, displayed in kilopascals. It works by generating a voltage difference difference between the measurement side, exposed to the atmosphere, and the non-measurement side, which is exposed to a permanently sealed, near-perfect vacuum. This measurement is integral to determining the density of the atmosphere inside of the lab.

6. Digital thermocouple

A digital thermocouple[3] is a digital measurement device that measures temperature, displayed in degrees Celsius. The device consists of two conductors of different metals - the hot and the cold junction. When the hot junction is heated, it generates a voltage proportional to the temperature difference between the plates. This measurement is integral to determining the density of the atmosphere inside of the lab.

7. Pressure transducer

The pressure transducer works in a similar way to the absolute pressure transducer described above, but measures the difference between two pressure values, and writes a proportional output in volts. One side of this device reads the stagnation pressure, while the other side reads the static pressure. The measurement obtained from this device is a gauge pressure.

8. Micro-manometer

A micro-manometer[4] is an analog measurement device used to measure pressure, displayed in inches of water. It operates on the principal of hydrostatic equilibrium, which states that the pressure exerted by a column of fluid is proportional to its height and density. The pressure being measured causes a column of water to rise to fall in a clear tube. Once equilibrium is reached and the meniscus is centered between the inscribed lines, a measurement of static gauge pressure drop across the contraction may be taken.

9. Scannivalve

A Scannivalve[5] is a digital measurement device similar to the transducer, and is used to measure pressure at multiple different locations, or 'ports'. It consists of a single transducer and a mechanism that switches the port as needed. This allows for smaller error, as a single machine can read at multiple different points. This measurement provides gauge pressure at several points across the test section.

10. Pitot tube

A pitot tube[6] is a physical tube-shape object with a central hole down the length of the tube and several holes drilled around the outside of the tube. These holes are kept separate, and the pressure transducer is connected across these holes to read the difference, i.e. the dynamic pressure. This is the device connected to the pressure transducer. There is a 90 degree bend present to normalize any disrupting airflow inside the tube.

III. Procedure

A. Data Collection

1. Part 1: Ambient Air Pressure and Density

For the first part of the data collection, the ambient air density must be determined. This is done by taking measurements of the dynamic pressure and the velocity inside the wind tunnel, using the pitot tube. The governing equation here is the equation for dynamic pressure, Eq.(6), which relates this pressure to the air flow velocity and density.

$$p = \frac{1}{2}\rho V_\infty^2 \tag{6}$$

This equation can be rearranged to solve for the fluid density of the steady flow aft of the airfoil, Eq. (7).

$$\rho = \frac{2p}{V_\infty^2} \tag{7}$$

The error associated with this measurement is found using Eq.(8), derived from Eq.(4), the partial derivatives of Eq.(7) w.r.t. p and V_∞, and the known or converted machine errors, δp and δV_∞. Note that the error δV_{infty} was found from Lab 1, in which the calibration procedure error calculations included pressure transducer transducer uncertainty for 40 Hz fan speed.

$$\delta\rho = \sqrt{\left(\frac{2}{V_\infty^2}\delta p\right)^2 + \left(-\frac{4p}{V_\infty^3}\delta V_\infty\right)^2} \tag{8}$$

If we are continuing to work under the assumption that the density of flow air and static air are the same, this density information holds and allows us to measure the absolute pressure, since density is typically calculated from the absolute pressure transducer and the digital thermocouple measuring static lab air. We can then use the ideal gas law, Eq.(9) to determine the absolute pressure:

$$p = \frac{m}{V}\frac{R}{M}T \tag{9}$$

Rearranging to use density, the result is Eq.(10), which relates pressure, density, and temperature with a known constant value specific to air.

$$p = \rho R T \tag{10}$$

The error associated with this measurement is found using Eq.(11), derived from Eq.(4), the partial derivatives of Eq.(10) w.r.t. ρ and T, and the known machine errors, $\delta\rho$ and δT.

$$\delta p = \sqrt{(287T \cdot \delta\rho)^2 + (287\rho \cdot \delta T)^2} \tag{11}$$

2. Part 2: Hot Wire Calibration

The first step is to calibrate the new instrument, the hot wire anemometer. This is done by centering the anemometer and stepping the fan speed up from 10Hz - 50Hz, in increments of 5Hz. This data is used later to plot the pitot tube flow velocity as a function of hot wire voltage and extract the needed coefficients for Kings law.

3. Part 3: Wind Tunnel Testing

First, the 0012 airfoil is mounted in the wind tunnel at its zero-lift angle of attack, 0° such that it is most streamlined and pressure differential over the surfaces is minimized. This allows us to determine how much of an effect skin drag has on an airfoil compared to pressure drag. According to the thin airfoil theory, a symmetric airfoil produces zero drag and zero lift at 0°. Thus, nearly all drag measured using through conservational laws can be attributed to the friction.

Operate the wind tunnel at a steady 40Hz fan speed. Using the hot wire, ensuring that it is first properly zeroed, move the hot wire from 0 steps to a final 14,000 steps in the following increments seen in Tab1:

Increment	Upper Step Limit
400	3,200
200	4,200
100	5,400
200	6,400
400	10,000
1,000	14,000

Table 1 Hot wire steps for NACA 0012 procedure

Measure the step number, pressures, pitot tube velocity, and temperature at each of these incremental steps. Save the data to process later.

The same needs to be done with the NACA 4412 airfoil, also mounted at its zero-lift angle of attack, which is roughly $-4°$. The incremental steps for this airfoil are similar, but slightly altered toward the middle to gather accurate data, as seen below in Tab.2

Increment	Upper Step Limit
400	4,000
200	5,200
100	6,000
200	7,200
400	10,000
1,000	14,000

Table 2 Hot wire steps for NACA 4412 procedure

B. Data Processing

1. Part 1: Calibration

Declare all global variables, including R_{air}, the manometer bias, the provided machine errors, the contraction area ratio, and symbolic variables ρ, V, P, and T. Define anonymous functions for Eq.(7) and Eq.(10) using these symbolic variables.

Import the data from the calibration file and extract the columns for temperature, pressure, hot wire voltage, and flow velocity. Next, plot the raw velocity vs voltage, and determine a line of best fit. For this case, it is best to linearize the graph by plotting the natural log of both the velocity and voltage and determining the slope and y-intercept of the linearized data. This is done in MATLAB with `log()` to convert the data, and then using `polyfit()` with a 1st order fit to determine the slope and y-intercept. Both the graph of the raw data and the linearized data can be seen below in Fig.2: From the coefficients determined by `polyfit()` for the line, apply Kings law, Eq. 5 to determine an equation which can be used to convert the hot wire voltage to velocity.

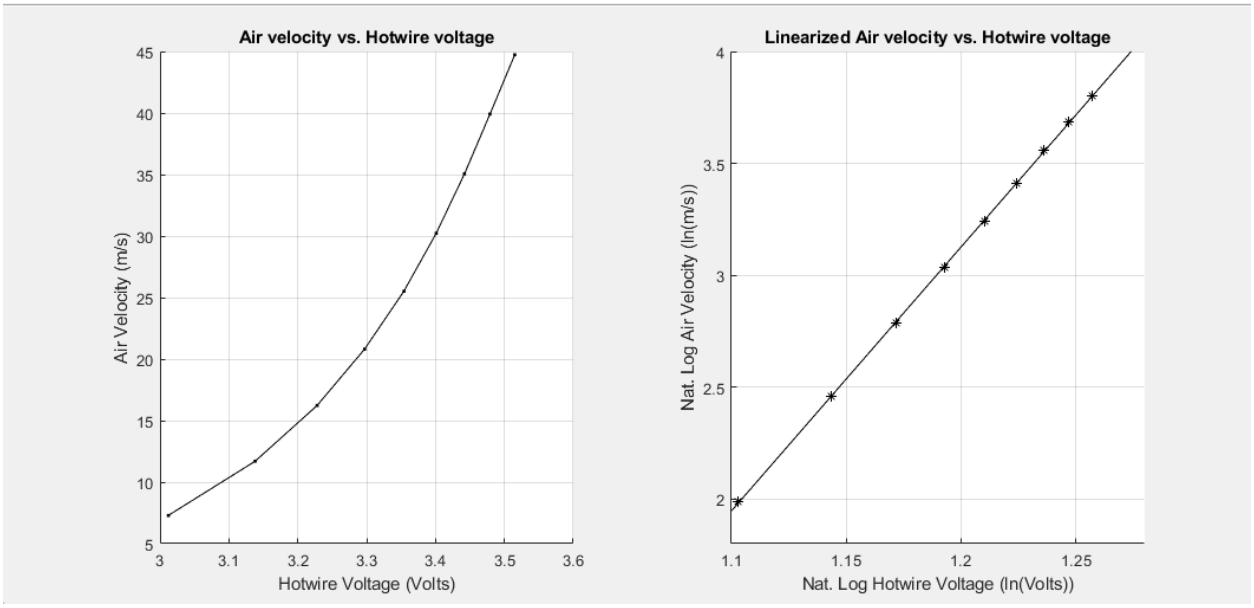

Fig. 2 Enter Caption

2. Part 2: Downstream Velocity Profile

Import the data from the 0012 and 4412 file using `importdata()`, and extract the needed data from the files, including all of the above columns, plus the static pressure drop and the hot wire steps. Use an anonymous function to determine the density at every data iteration from the velocity and the dynamic pressure. Then use the density value to determine the absolute pressure. Since both of these are measured at steady state flow and the variation is minimal, the average values can be taken. The error in these measurements can then be found using the equations Eq.8 and Eq.11.

From the data file voltage measurements, the velocity profile behind the airfoil can be measured, alongside the linear calibration coefficients and Kings law. Both the numerical and normalized velocity profile were plotted. For the normal graph, each data point for the y-location and the velocity were divided by the maximum value to obtain a number between 0 and 1. For the numerical graph, the steps were converted to meters, and the velocity was left alone. To convert steps to meters, it is known that there are 400 steps in one revolution and 16 revolutions in one inch. From there, inches can be converted into meters and plotted on the y-axis.

3. Part 2: Drag Calculations

First, note that, while the following integrals are computed across the area of the inlet and exit control volume surfaces, the purpose of this experiment is to determine the *section* drag coefficient, and thus, all computations are finding the force or drag per unit width, and as such, the values solved for are in one dimension. The first step for determining the drag is to define a control volume. For these purposes, let it be limited on the top and bottom by a streamline, such that no flow crosses the boundary. If the left side control volume is the height in meters of the total hot wire range, the inlet height can be determined using mass conservation. The equation for mass conservation can be seen below:

$$\int_{CS} \rho(\vec{V} \cdot \hat{n})\, dA = 0 \tag{12}$$

Performing this integration with the downstream velocity profile along the exit will determine how much mass is leaving the control volume. This number can then be equated to the mass at the entrance of the control volume, taking the average of the pitot tube velocity and the average flow density. This will yield an entrance height which is ever so slightly smaller than the exit height.

Next, with the fully defined control volume, the conservation of momentum can be applied to determine the total force exerted on the fluid, which is equal and opposite to the force the fluid exerts on the airfoil. Since both airfoils are mounted at their respective zero-lift angle, all the force that the fluid exerts on the airfoil can be attributed to the drag

force. The equation for momentum conservation is as follows:

$$\int_{CS} \rho V(\vec{V} \cdot \hat{n})\, dA = 0 \tag{13}$$

Note that there is no term in this momentum conservation for the pressure times the control surface area. This is because the pressure is the same everywhere, and the forces inevitably cancel out in all directions. This leaves us with simply the above expression at the inlet and exit of the control volume. This equation can be broken down into the following to determine the force in the x-direction on the fluid:

$$F_x = -\int_1 \rho V_1(\vec{V}_1 \cdot \hat{n})\, dA_1 + \int_2 \rho V_2(\vec{V}_2 \cdot \hat{n})\, dA_2 \tag{14}$$

From this equation, the coefficient of drag per unit width can be found by making the force dimensionless, i.e. dividing by the dynamic flow pressure and the chord length, as seen in Eq.15 below:

$$C_d = \frac{d}{q_\infty c} \tag{15}$$

IV. Results

After linearization of the calibration curve for the flow velocity vs hot wore voltage, the coefficients for m and b were determined, as seen in Tab.3:

m	b
11.7968	-11.0300

Table 3 Linear coefficients from the calibration procedure

These are the coefficients used in Eq. 5 to determine the wake velocity profile of the airfoils, yielding the following calibration curve for converting voltage to velocity, Eq.16:

$$V = E^{11.7968} \cdot e^{-11.0300} \tag{16}$$

This was used to produce the wake profile, as seen below for NACA 0012 and NACA 4412 respectively:

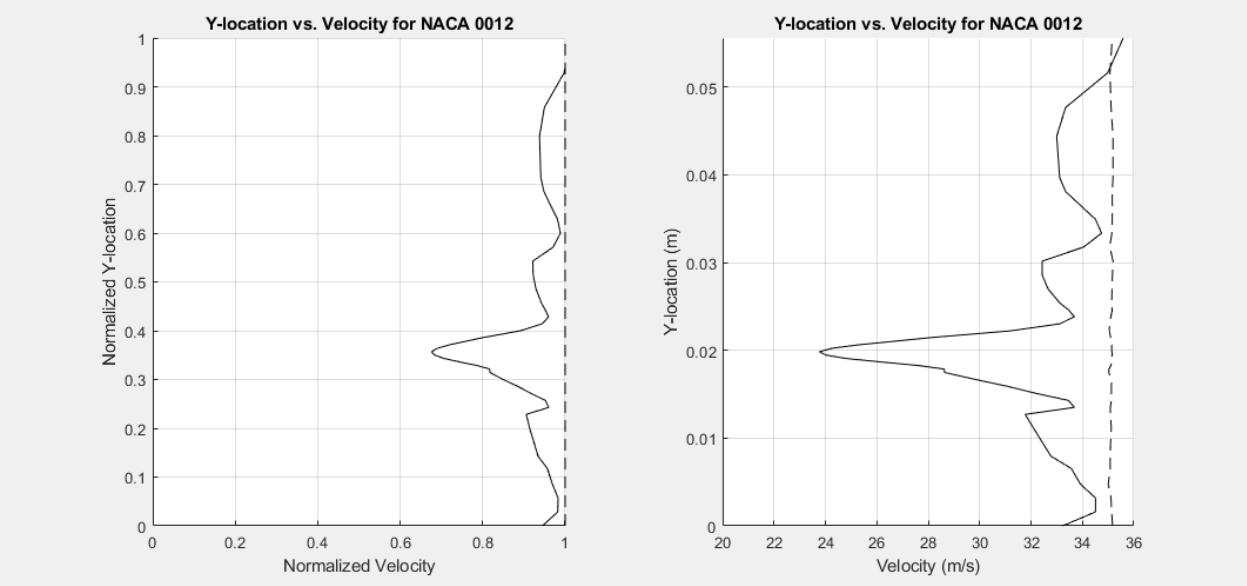

Fig. 3 Normalized wake profile and dimensional wake profile for NACA 0012. Note the overall general symmetry

Airfoil	Inlet Size (m)	Outlet size (m)
0012	0.0519	0.0556
4412	0.0513	0.0556

Table 4 Inlet and outlet size for each control volume

Airfoil	Drag force (N)	Drag Coefficient
0012	4.3156	0.0636
4412	4.7397	0.0705

Table 5 Drag and drag coefficient per unit width for both the NACA 0012 and 4412.

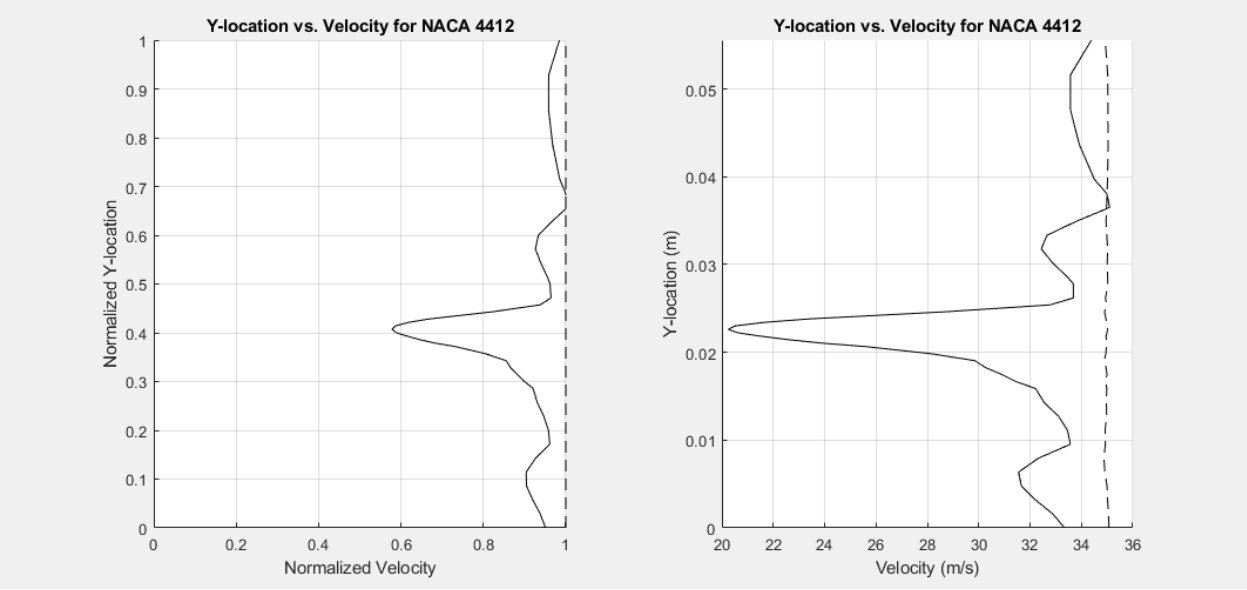

Fig. 4 Normalized wake profile and dimensional wake profile for NACA 4412. Note the lack of overall symmetry relative to NACA 0012

The exit mass for both airfoil tests was computed to find the control volume inlet size to maintain mass conservation. The values can be seen below in Tab.4: Next, the momentum conservation equation was computed in steady state form for the entrance and in integral form for the exit. This yields a negative value for the external force, which is expected, as the mass conservation equation determined the force on the fluid due to an external object in the control volume. The force *on* the object, in this case, the drag, is equal and opposite according to newton. This is the force that will be used in Eq.15 to determine the drag per unit width. After making these computations, the following values were determined, seen in Tab5 Note that the chord length here is 100mm, or 0.1m. The entrance dynamic pressure was used, and was averaged across all data points taken.

V. Conclusion

These results can then be compared with the measurements from the previous lab and from outside sources like Abbot's theory of wing sections, [7]. The following is a figure for the drag measured by Abbot for the NACA 0012:

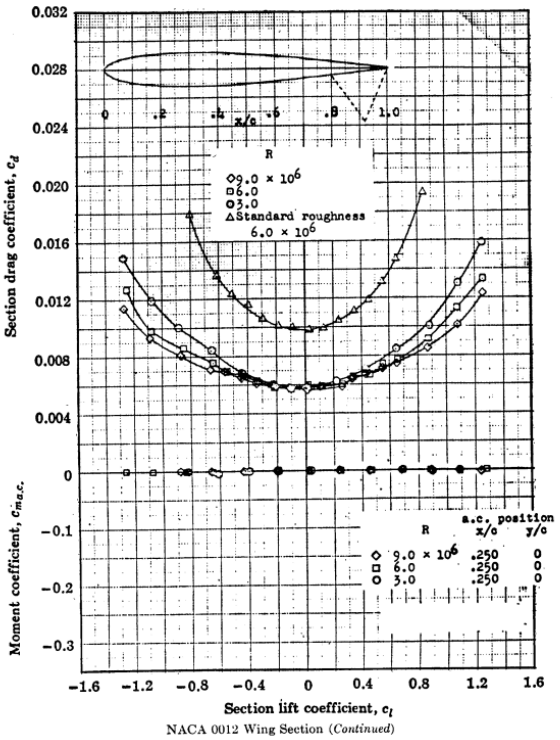

NACA 0012 Wing Section (*Continued*)

Fig. 5 Enter Caption

This graph from Abbot shows that the NACA 0012 should have a nearly-zero drag coefficient at a zero-lift angle of attack, which would make sense considering only the pressure drag. The airfoil tested has real skin friction considerations and is working at a relatively low Reynolds number, so it is typically expected that our test will produce more drag. Our test of NACA 0012 resulted in a drag coefficient that is bigger by over 6.5 times than the largest drag coefficient reported by Abbot. Compared to the previous lab and homework values, this lab figure is larger by a factor of almost 22 times. This is generally expected, as according to thin airfoil theory, at zero-lift angle of attack, there is neither lift nor drag produced for a symmetric airfoil. As such, the values from previous labs and homework would result in a significantly smaller number for drag, as it was computed according to thin-airfoil theory.

The NACA 4412 produced slightly more drag, which is to be expected in this case. It is a slightly less streamlined due to the camber, and while it is still mounted at the zero-lift angle of attack, the lesser streamline nature means that the flow will lose more momentum as it interacts with the surface of the body. The NACA 4412 produces a little over 10% more drag due to friction here, with a C_D of 0.0705.

From these results, it can be seen that the friction drag actually contributes a very large portion of the drag on an airfoil, and should not be neglected in airfoil design and testing. This shows that, while the thin airfoil theory is a good predictor of behavior, conservational analysis should still be used to obtain accurate numerical data for airfoil and body design.

It is important to note that drag is not always a bad thing by any means. Drag is used to provide restoring force and stability to airborne bodies and is intentionally induced with control surfaces to make an aircraft controllable. From the perspective of raw lift-to-drag efficiency, this force should be minimized, but that is rarely the only concern, as most flying objects should harness this in some form or another to design manual or autonomous control systems.

Overall, the experiment successfully met the objective of analyzing the drag characteristics of standard airfoils at zero-lift angles of attack. Using the calibrated measurement instruments, specifically the hot wire anemometer and the density of lab air, the wake profile was measured and used in accordance with conservation laws to determine just mow much flow momentum is lost due to the combined pressure and frictional drag

Some potential sources of error are, of course, the known machine error. Aside from this, Other sources include the human error in setting the angle of attack, since it was done using a protractor attached to the airfoil. This is completely

down to human accuracy, which could introduce some uncertainty. Rounding error is unlikely, since the computations were performed using computer software. The hot wire can produce some sources of wake profile error, as it is very sensitive to things like vibration, flow temperature variation, and a relatively limited range of data collection. This would have an impact on the conservation computations, as this data is directly used to determine the mass and momentum outflow.

VI. Acknowledgments

I would first like to thank my lab TA for the beautiful figures and guidance throughout the experiment. I would also like to thank Monster Beverage Corporation for providing me with the necessary caffeine to get through this week. I just really wish they would lower their prices. Lastly I would like to thank my cat Robby for the moral support he provided, i.e. screaming outside my door whenever I did not let him watch me do my homework and step on my keyboard.

References

[1] NASA, "Low speed tunnel operation," , 2021. URL https://www.grc.nasa.gov/www/k-12/airplane/tunop.html.

[2] Craig, B., "What is absolute pressure transmitter [and] how does it work?" , Jul 2023. URL https://www.transmittershop.com/blog/absolute-pressure-transmitter-working-principle-applications/#:~:text=Simply%2C%20the%20side%20of%20the,mechanical%20energy%20into%20electrical%20signals.

[3] munroscientificdivision, 2024. URL https://www.munroscientific.co.uk/a-guide-for-laboratory-thermometer#:~:text=A%20laboratory%20thermometer%20is%20an,scale%20that%20indicates%20the%20temperature.

[4] click2electro, "Manometer Basics & Micromanometer," , Apr 2023. URL https://click2electro.com/forum/instrumentation-measurement/manometer-basics-micromanometer/.

[5] links open overlay panelGiuseppe P. Russo, A., and chapter highlights pressure sensors ranging from the classical manometers, A., "Pressure sensors," , Mar 2014. URL https://www.sciencedirect.com/science/article/pii/B9781845699925500012.

[6] NASA, "Pitot tube," , 2024. URL https://www.grc.nasa.gov/www/k-12/VirtualAero/BottleRocket/airplane/pitot.html.

[7] H.Abbott, I., and Doenhoff, A. E., "Theory of Wing Sections," , 1949. URL https://canvas.asu.edu/courses/200674/files/92667810?module_item_id=14753595.